OPTOELECTRONICS AND ADVANCED MATERIALS – RAPID COMMUNICATIONS Vol. 1, No. 9, September 2007, p. 425 - 429

Linear and nonlinear optical properties of $SrBi_2Nb_2O_9$ thin films fabricated by RF magnetron sputtering

KANSONG CHEN*, HAOSHUANG GU, LI XU
School of Physics and Electronic Technology, Key Laboratory of Ferroelectric and Piezoelectric Materials and Devices of Hubei Province, Hubei University, Wuhan 430062, China

$SrBi_2Nb_2O_9$ (SBN) thin films were prepared on fused quartz substrates at room temperature by RF magnetron sputtering technique. The structure and the composition of the films were characterized by X-ray diffraction and X-ray fluorescence spectrometry. The optical transmittance of the samples was measured and their dispersion of refractive index was found to follow the Sellmeier-type dispersion relation. The nonlinear optical properties of the films were determined using a single beam z-scan technique at a laser wavelength of 532 nm with duration of 25 ps. The real and imaginary parts of the third-order nonlinear optical susceptibility $\chi^{(3)}$ were -6.10×10^{-8} esu and 1.94×10^{-8} esu, respectively, suggesting a self-defocusing optical nonlinearity. The results show that SBN thin films have great potential applications in nonlinear optics.

(Received July 31, 2007; accepted August 15, 2007)

Keywords: $SrBi_2Nb_2O_9$ thin films, RF magnetron sputtering, Optical transmittance, Nonlinear optical properties, Z-scan technique

1. Introduction

Bismuth layered ferroelectrics, which have high fatigue resistance and are able to withstand 10^{12} erase/rewrite operations, are leading candidate materials for use in nonvolatile random access memory (NvRAM) applications and have attracted considerable attention [1,2]. As one of Bi-layered compounds, $SrBi_2Nb_2O_9$ (SBN) belongs to the Aurivillius type structure consisting of Bi_2O_2 layers and perovskite-type $SrNb_2O_7$ units with double NbO_6 octahedral layers [3]. Till now, a lot of research works on the basic structure and the enhanced dielectric and ferroelectric properties of SBN materials have been successfully carried out. Zurbuchen et al. [4] reported the ferroelectric domain structure of SBN epitaxial thin films. Shimakawa et al. [5] found that the orbital hybridization and covalency play important roles in the ferroelectric properties of SBN materials. Forbess et al. [6] reported the influences of Ca^{2+} and La^{3+} doping on the electrical properties of SBN ceramics. Gu et al. [7] observed the significant dielectric enhancement in $0.3BiFeO_3$-$0.7SrBi_2Nb_2O_9$. On the other hand, the nonlinear optical properties of ferroelectric thin films, recognized to be important from the optical device point of view, have been studied in recent years. It is reported that large optical nonlinearities have been exhibited in some ferroelectric thin films, such as Ce: $BaTiO_3$, $Pb_{0.95}La_{0.05}Zr_{0.53}Ti_{0.47}O_3$, Nd-substituted $Bi_4Ti_3O_{12}$ ($BNT_{0.25}$), $Ba_{0.7}Sr_{0.3}TiO_3$, and $Bi_{3.25}La_{0.75}Ti_3O_{12}$ [8-12]. Thus, a fundamental understanding of the linear and nonlinear optical properties of SBN thin films is also quite necessary for applications in optoelectronic devices. However, less effort has been directed to these up till now.

Recently, a variety of thin-film growth techniques, including metalorganic solution deposition process (MOD) [13], pulsed laser deposition (PLD) [14], and sol-gel method [15], were successfully used to prepare SBN thin films. Compared with these methods, magnetron sputtering for thin-film preparation has many advantages such as low temperature processing, good homogeneity, simple processing procedures, and low cost [16]. In this paper, we report on the experimental investigation of linear and nonlinear optical properties of SBN films on fused quartz substrates using RF magnetron sputtering technique.

2. Experimental

The SBN thin films were deposited by RF magnetron sputtering, which took place in a JGP560CV sputtering system made of stainless steel cylinder. The SBN ceramic target was a disk of diameter 60 mm and placed on a circular magnetron pedestal on the floor of the chamber. The substrate was mounted in a holder 52 mm vertically above the target. Prior to film deposition, the plasma chamber was evacuated to less than 4×10^{-4} Pa by a turbomolecular pump. Then the target was pre-sputtered alone for 15 minutes to cleanse the surface contamination layer, during which the substrates were covered with a moveable shield. A sputtering gas mixture of O_2/Ar in the ratio 3:1 and total pressure 2.4 Pa was used throughout. A three-channel mass flow controller was used to control independently the injection rates of Ar and O_2. The sputtering took place at an RF frequency of 13.56 MHz and discharge power of 150 W. The films were grown at

room temperature for 2 hours and then annealed at 700 ^{o}C for 1 hour in the presence of pure O_2 gas.

The crystalline structure and crystallographic orientation of the SBN thin films were analyzed by Rigaku D/Max-3C X-ray diffraction using CuKα radiation (λ=0.154056nm) as the radiation source. The composition and chemical stoichiometry of the samples was characterized by Shimadzu XRF-1800 spectrometer with RhKα x-ray tube as excitation source. The optical transmittance of the thin films was measured with a Perkin-Elmer Lambda 17 UV/VIS spectrophotometer in the wavelength range from 300 to 800 nm.

The third-order nonlinear optical properties of the SBN films were determined by z-scan method that it immediately indicates the sign and type of nonlinearity (nonlinear refraction and nonlinear absorption) [17]. The sample is moved along the z-axis of the focused Gaussian-profile laser beam, the power of which is kept constant during the whole scan. In our experiments, a *Q*-switched Nd:YAG laser with a wavelength of 532 nm and the pulse width of 25 ps was employed as the light source. The light beam was a TEM00-mode optical Gaussian spatial profile and focused by a lens with a focal length of 120 mm. The radius of the beam waist (ω_0) was 26.8 μm, which is calculated from the equation $\omega(z)^2=\omega_0^2(1+z^2/z_R^2)$, where $z_R= \pi\omega_0^2/\lambda$ is the Rayleigh length. Hence, the value of z_R is calculated to be 4.2 mm, much longer than the thickness of either substrates or films. The reference beam energy and the on-axis transmitted beam energy through an open-aperture (OA) or a closed-aperture (CA) were simultaneously measured by an energy ratiometer (Rm6600, Laser Probe Corp.). The linear transmittance of the pulse energy passing the aperture to the total energy was measured to be 0.1 without sample loaded. The CA detector is sensitive both to the nonlinear refraction and to the nonlinear absorption, the OA detector only to the latter. During z-scan measurement, two identical photodetectors and an energy ratiometer were used to eliminate the influence of the laser power fluctuation by dividing the transmitted power by the power obtained at the reference detector. Furthermore, the laser repetition rate was set to 1Hz to reduce the possible thermal accumulative effect, and a transmission of the sample was calculated by averaging 20 pulses.

3. Results and discussion

3.1. Structure and composition

Fig. 1 shows the X-ray diffraction pattern of the SBN thin films grown on fused quartz substrates. As can be seen, the thin films presented polycrystalline structure and were crystallized into SBN phase with (115), (200), and (2010) peaks appearance. The lattice constants a, b, and c were calculated to be 5.486 Å, 5.475 Å, and 24.934 Å, respectively, approximately equal with the values of 5.518 Å, 5.515 Å, and 25.112 Å shown on JCPDS File 86-1190, indicating that the films have a single phase of layered perovskite structure without presence of secondary phase.

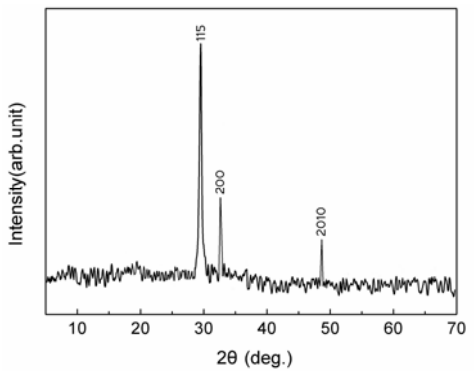

Fig. 1. XRD pattern for SBN thin films grown on fused quartz substrates.

The composition of the samples was characterized by X-ray fluorescence spectrometry. Fig. 2 shows the XRF pattern of the SBN films using fundamental parameter (FP) method with RhKα x-ray tube as excitation source, which reveals that the samples contain Strontium (Sr), Bismuth (Bi), and Niobium (Nb) cations in a 1:1.92:1.98 ratios, and have very small deviation from chemical stoichiometry of SBN.

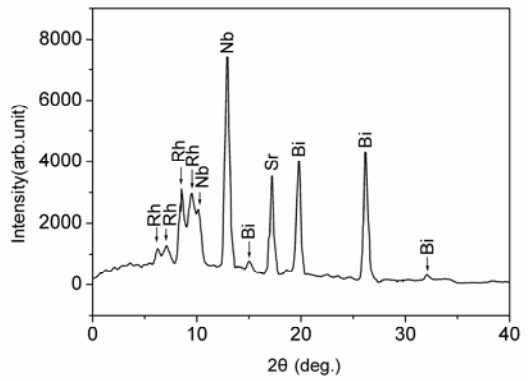

Fig. 2. XRF spectrum of SBN thin films using fundamental parameter (FP) method with RhKα X-ray tube as excitation source.

3.2. Linear optical properties

Fig. 3 shows the optical transmission spectrum for the SBN thin film annealed at 700 ^{o}C in the wavelength range of 300 - 800 nm. The film exhibits a sharp absorption edge and good transparency to the light of wavelength bigger than 390 nm. The oscillations in transmittance result from reflection from the top surface of the film and the interface between the film and substrate. The well oscillating optical transmittance suggests that the as-prepared film has a flat surface and a uniform thickness. The linear refractive index n_0, absorption coefficient α, and the thickness of the thin film can be obtained from the transmission curve by using the method proposed by Manifacier et al. [18]. Fig. 4 shows the dispersion curve of

the refractive indices of SBN thin film in the wavelength range of 390 - 740 nm. The dispersion curve is fairly flat above 550 nm and rises rapidly towards the shorter wavelength region, showing the typical shape of a dispersion curve near an electronic interband transition [19]. The n_0 and α were calculated to be 2.21 and 1.17×10^3 cm^{-1} at the wavelength of 532 nm, respectively. The thickness of the film calculated in this way was about 0.572 μm, nearly equal to the measured value 0.58 μm.

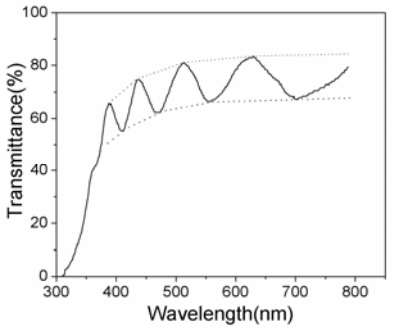

Fig. 3. The optical transmission spectrum of SBN thin films annealed at 700^o C on fused quartz substrate.

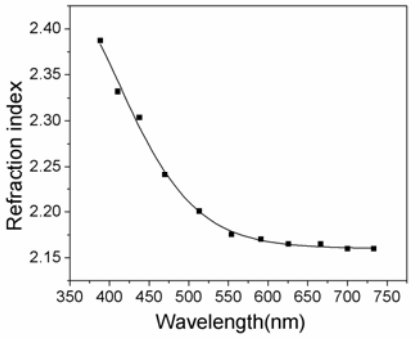

Fig. 4. The wavelength dispersion curve of the refractive index of SBN thin films.

Dispersion data in the interband transition region are most often analyzed using a single electronic oscillator model proposed by DiDomenico and Wemple [20]. The dispersion of the refractive index can be described by the Sellmeier dispersion formula

$$n^2 - 1 = \frac{s_0 \lambda_0^{\ 2}}{1 - (\lambda_0 / \lambda)^2} \tag{1}$$

where λ_0 is an average oscillator wavelength and s_0 is the average oscillator strength. The variation of $1 / (n^2-1)$ with $1 / \lambda^2$ have been plotted for SBN film in Fig. 5. The plot gives a straight line, and fits the Sellmeier dispersion formula with a single electronic oscillator well. From the linear relation shown in Fig. 5, the values of S_0 and λ_0 were calculated to be 0.709×10^{14} m^{-2} and 0.214 μm, respectively. We can further obtain the average oscillator energy E_0 ($E_0 = hc/\lambda_0$) and the refractive index dispersion parameter E_0/S_0, which depends on the characteristics of the interband transitions. The values are 5.809 eV and 8.191×10^{-14} eV m^2 for SBN thin film on fused quartz substrate, respectively.

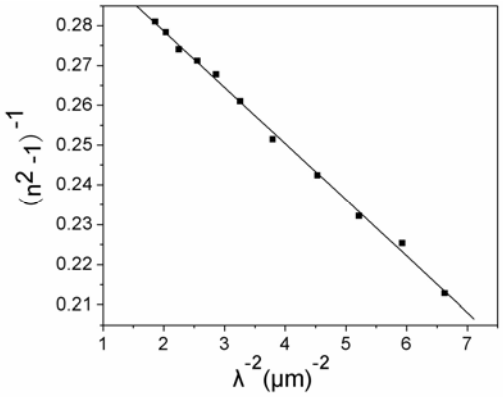

Fig. 5. The variation of $1 / (n^2-1)$ of SBN thin films with $1/\lambda^2$.

At shorter wavelength close to the optical band gap, the transmittance T with absorption coefficient α follows the simple relation [21]

$$T = A \exp(-\alpha d) \tag{2}$$

where A is nearly equal to unity at the absorption edge, and d is the thickness of the films. The band gap energy (E_g) can be estimated by assuming a direct transition between valence and conduction bands. Above the threshold of absorption, the dependence of α on incident photon energy hν is given by the expression [22]

$$(\alpha h\nu)^2 = k \times (h\nu - E_g) \tag{3}$$

where k is a constant. The optical band gap E_g can be found by fitting $(\alpha h\nu)^2$ versus hν to the experimental data of the film (see Fig. 6). From the linear part of the dependence, supporting the assumption of a direct transition, the extrapolated band gap E_g was obtained to be 3.58 eV.

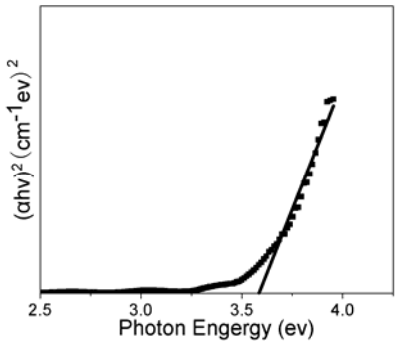

Fig. 6. The plot of $(\alpha h\nu)^2$ vs. hν for SBN thin films at annealing temperature of 700 ^{o} C.

3.3. Third-order optical nonlinearity

Typical open-aperture (OA) and closed-aperture (CA) z-scan profiles for the SBN thin films are shown in Fig. 7 (a) and (b), respectively. The solid lines are theoretical fits. It is obvious from Fig. 7 (a) that the OA curve for the samples comprises a normalized transmittance valley, indicating the presence of nonlinear absorption in the SBN films. In order to obtain nonlinear refraction information in the CA z-scan experiment, the measured closed-aperture transmittance was divided by the corresponding open-aperture data. The CA curve with a peak-to-valley shape in Fig. 7 (b) indicates that the sign of the nonlinear refractive index n_2 is negative, i.e. self-defocusing occurs. The high nonlinear optical properties result from the SBN films because the fused quartz substrate has a very small nonlinear optical response at 532 nm. The measurements were performed at several intensities, and the variation of Δn with different peak input irradiance I_0 exhibits a linear relation, which implies that the observed nonlinear effect is a third-order response. This can also be verified from the fact that the peak and valley are separated by about 8 mm as compared to 1.7 z_R in Fig. 7 (b).

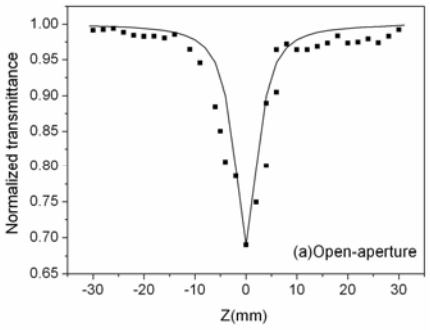

a

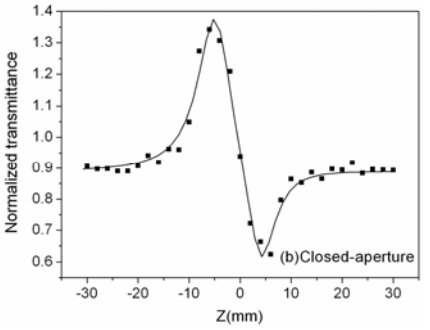

b

Fig. 7. (a) Open-aperture and (b) closed-aperture z-scan measured curves of SBN films. The solid lines are the theoretical fits.

The data were analyzed using the procedures described by Sheik-Bahae et al [17]. The nonlinear absorption coefficient β (m/W) can be estimated from the OA z-scan data. The normalized transmittance for the open-aperture is given by

$$T(z, s=1) = \sum_{m=0}^{+\infty} \frac{(-\beta I_0 L_{eff})^m}{(m+1)^{3/2}} \tag{4}$$

where I_0 is the intensity of the laser beam at the focal point, $L_{eff}=1-\exp(-\alpha L)/\alpha$ is the effective thickness of the film, α is the linear absorption coefficient, and L is the thickness of the film.

The nonlinear refractive index n_2 can be obtained through CA z-scan measurement by the following expression

$$n_2(esu) = \frac{cn_0}{40\pi^2} \frac{\lambda \Delta T_{P-V}}{0.812(1-s)^{0.25} L_{eff} I_0} \tag{5}$$

where ΔT_{p-v} is the normalized transmittance difference between peak and valley as shown in Fig. 7 (b), n_0 is the linear refractive index of the sample, λ is the light wavelength, and S is the linear transmittance of the aperture.

The calculated values of β and n_2 of the SBN films are 3.70×10^{-7} m/w and -2.60×10^{-7} esu, respectively. Furthermore, The real and imaginary parts of the third-order nonlinear optical susceptibility $\chi^{(3)}$ can be obtained according to the following equations

$$\mathrm{Re}\,\chi^{(3)}(esu) = \frac{n_0}{3\pi} n_2(esu) \tag{6}$$

$$\mathrm{Im}\,\chi^{(3)}(esu) = \frac{{n_0}^2 c^2}{240\pi^2 \omega} \beta(m/W) \tag{7}$$

where ω is the angular frequency of the light field. The values of Re $\chi^{(3)}$ and Im $\chi^{(3)}$ were calculated to be -6.10×10^{-8} esu and 1.94×10^{-8} esu, respectively. The absolute value of $\chi^{(3)}$ was found to be 6.40×10^{-8} esu ($\left|\chi^{(3)}\right| = \sqrt{(\mathrm{Re}\,\chi^{(3)})^2 + (\mathrm{Im}\,\chi^{(3)})^2}$).

The magnitude of $\chi^{(3)}$ of SBN thin films is high and comparable with that of other representative nonlinear optical thin-film materials (see Table 1) [8,11,23,24], suggesting SBN thin film is promising for using in nonlinear optical devices, such as optical limiting, switching, and modulated-type optical devices. Generally, the nonlinear optical phenomena can be classified into the resonant- and nonresonant-based nonlinear effects depending upon whether virtual or real states are involved in optical excitation [25]. The nonlinear refractive index would be changed by different physical actions, such as distortion in Electron distribution, optical Kerr effect, electrostrictive effect, and thermal-optical effect. Their contribution to the nonlinear refractive index depends on the duration of incident light since they have different response time. For pulsed laser with duration of picosecond time scale in our experiment, the optical nonlinearity of SBN films is mainly derived from the distortion in electronic cloud distribution. Contribution of other physical actions can be ignored due to their much slower response time (nanosecond or longer). In this work,

the negative sign of the nonlinear refractive index n_2 indicates the resonant electronic transition process causes the self-defocusing optical nonlinearity in SBN thin films, whose contributions to the change of the refractive index can cancel the positive nonresonance contributions. The negative sign of n_2 gives evidence of the electronic origin of the optical nonlinearity in SBN thin films. Furthermore, when the resonances are used to enhance the optical nonlinearity in condensed matter, the resonant interactions can occur, which involve real electronic transitions.

Table 1 Values of $\chi^{(3)}$ of several representative nonlinear optical thin films.

Films	$\chi^{(3)}$ (esu)	References
$SrBi_2Nb_2O_9$	6.40×10^{-8}	This work
Ce: $BaTiO_3$	2.21×10^{-8}	[8]
Cu: $Ba_{0.5}Sr_{0.5}TiO_3$	9.74×10^{-9}	[11]
Au: SiO_2	1.60×10^{-8}	[23]
Cu: Al_2O_3	2.06×10^{-8}	[24]

4. Conclusions

SBN thin films with bismuth-layered perovskite structure were deposited on fused quartz substrates by RF magnetron sputtering technique. The relation between the refractive index of the SBN films and wavelength was found to follow Sellmeier dispersion formula from the optical transmittance measurements. In addition, the optical constants of the films were obtained, such as the band gap of 3.58 eV, the linear refractive index of 2.21 at 532 nm, and the linear absorption coefficient of 1.17×10^3 cm^{-1}. The third-order nonlinear optical properties of the SBN films were determined by the z-scan technique. The nonlinear absorption coefficient and refractive index were measured and their values are 3.70×10^{-7} m/W and -2.60×10^{-7} esu, respectively, indicating the self-defocusing optical nonlinearity. The calculated values of Re $\chi^{(3)}$ and Im $\chi^{(3)}$ were -6.10×10^{-8} esu and 1.94×10^{-8} esu, respectively. The results suggest that the SBN thin film is a promising candidate material for nonlinear optical applications.

Acknowledgements

This work was supported by the National Natural Science Foundation of China (50272020), the Youth Project of Wuhan Municipality of Hubei Province of China (20055003059-9) and the Excellent Innovation Research Team Project of Hubei Province of China.

References

[1] C. A. Paz de Araujo, J. D. Cuchiaro, L. D. McMillan, M. C. Scott, J.F. Scott, Nature **374**, 627 (1995).
[2] Auciello, J. F. Scott, R. Ramesh, Phys. Today **51**, 22 (1998).
[3] H. S. Gu, T. J. Zhang, W. Q. Cao, J. M. Xue, J. Wang, Mater. Sci. Eng. B **99**, 116 (2003).
[4] M. A. Zurbuchen, G. Asayama, D. G. Schlom, Phys. Rev. Lett. **88**, 107601 (2002).
[5] Y. Shimakawa, H. Kimura, S. Kimura, Y. Kubo, Phys. Rev. B **66**, 144110 (2002).
[6] M. J. Forbess, S. Seraji, Y. Wu, C.P. Nguyen, G.Z. Cao, Appl. Phys. Lett. **76**, 2934 (2000).
[7] H. S. Gu, J. M. Xue, J. Wang, Appl. Phys. Lett. **79**, 2061 (2001).
[8] W. S. Shi, Z. H. Chen, N. N. Liu, H. B. Lu, Y. L. Zhou, D. F. Cui, G. Z. Yang, Appl. Phys. Lett. **75**, 1547 (1999).
[9] W. F. Zhang, Y.B. Huang, M.S. Zhang, Appl. Surf. Sci. **158**, 185 (2000).
[10] Y. H. Wang, B. Gu, G. D. Xu, and Y. Y. Zhu, Appl. Phys. Lett. **84**, 1686 (2004).
[11] J.S. Kim, K.S. Lee, S.S. Kim, Thin Solid Films **515**, 2332 (2006).
[12] F. W. Shi, X. J. Meng, G. S. Wang, J. L. Sun, T. Lin, J.H. Ma, Y.W. Li, J.H. Chu, Thin Solid Films **496**, 333 (2006).
[13] X. F. Du, I.W. Chen, J. Am. Ceram. Soc. **81**, 3265 (1998).
[14] J. Lettieri, M.A. Zurbuchen, Y. Jia, D.G. Schlom, S.K. Streiffer, M.E. Hawley, Appl. Phys. Lett. **76**, 2937 (2000).
[15] S. M. Zanetti, E.R. Leite, E. Longo, J.A.Varela, J. Europ. Ceram. Soc. **19**, 1409 (1999).
[16] T. Miyazaki, T. Fujimaki, S. Adachi, K. Ohtsuka, J. Appl. Phys. **89**, 8316 (2001).
[17] M. sheik-Bahae, A.A. Said, T.H. Wei, D.J. Hagan, E.W. Van Stryland, IEEE J. Quantum Electron **26**, 760 (1990).
[18] J.C. Manifacier, J. Gasoit, J.P. Fillard, J. Phys. E. Rev. Sci. Instrum. **9**, 1002 (1976).
[19] M. Wohlecke, V. Marrello, A. Onton, J. Appl. Phys. **48**, 1748 (1977).
[20] M. DiDomenico, S.H. Wemple, J. Appl. Phys. **40**, 720 (1969).
[21] H.S. Gu, D.H. Bao, S.M. Wang, A.X. Kuang, Thin Solid Films **283**, 81 (1996).
[22] J. Callaway, Quantum Theory of the Solid State, Academic Press, New York (1974).
[23] M.Y. Lee, T.S. Kim, Y.S. Choi, J. Non-cryst. Solids **211**, 143 (1997).
[24] J.M. Ballesteros, R. Serna, J. Solis, C.N. Afonso, A.K. Petford-Long, D.H. Osborne, R.F. Haglund, Appl. Phys. Lett. **71**, 2445 (1997).
[25] X.H. Zhu, Q. Li, N.B. Ming, Z.Y. Meng, Appl. Phys. Lett. **71**, 867 (1997).

*Corresponding author: kschen1999@yahoo.com.cn